Revista de Informática Teórica e Aplicada - RITA - ISSN 2175-2745
Vol. 33, Num. 4 (2026) 44-52
RESEARCH ARTICLE

Computational Method for Continuous Monitoring of Ocular Artifacts in Electroencephalography Data

Método Computacional para Monitoramento Contínuo de Artefatos Oculares em Dados de Eletroencefalografia

Yuri S. Pereira[1,2]*, Daniel D. F. Luft[1,2], Matheus G. Tavares[1], Tadeu Vargas[1], Samuel S. Cardoso[1]

Abstract: This work presents a computational method for detecting ocular artifacts in *EEG/EOG* signals, focusing on *Brain-Computer Interfaces* and *Assistive Technologies*. The system uses an Arduino Nano and *AD8232* module for real-time acquisition and processing, implementing an algorithm based on voltage thresholds and signal derivative analysis. In a series of 15-minute trials across 4 patients (totaling 60 minutes of data), 992 blinks were detected, of which 840 were real and 152 false, with only 24 missed. The method achieved an precision of 84.7% and a sensitivity of 97.2%, demonstrating effectiveness in identifying real blinks and potential for *EEG* pre-processing and assistive control applications.
Keywords: EEG — EOG — ocular artifacts — real-time processing — assistive technology

Resumo: Este trabalho apresenta um método computacional para detecção de artefatos oculares em sinais de EEG/EOG, com foco em interfaces cérebro-computador e tecnologias assistivas. O sistema utiliza Arduino Nano e módulo AD8232 para aquisição e processamento em tempo real, aplicando um algoritmo baseado em limiares de tensão e derivada do sinal. Em ensaios de 15 minutos realizados com 4 pacientes (totalizando 60 minutos de dados), foram detectadas 992 piscadas, sendo 840 reais e 152 falsas, com apenas 24 não identificadas. O método alcançou precisão de 84.7% e sensibilidade de 97.2%, demonstrando eficácia na identificação de piscadas reais e potencial para aplicações em pré-processamento de EEG e controle assistivo.
Palavras-Chave: eletroencefalografia — eletro-oculografia — artefatos Oculares — Processamento em Tempo Real — tecnologia assistiva

[1] *Instituto Federal de Educação, Ciência e Tecnologia Sul-rio-grandense (IFSul), Brazil*
[2] *Universidade Federal de Santa Maria (UFSM), Brazil*
Corresponding author: yurisilveirapereira@gmail.com
DOI: http://dx.doi.org/10.22456/2175-2745.150325 • **Received:** 19/09/2025 • **Accepted:** 27/06/2026

1. Introduction

The detection of ocular blinks is the central focus of this study, with potential applications in assistive devices through *Brain-Computer Interfaces* (*BCI*) and *Electrooculography* (*EOG*), as well as for improving the quality of *Electroencephalography* (*EEG*) signals. In the context of assistive technologies, such as wheelchair control, voluntary blinks can be converted into precise commands, offering greater autonomy to individuals with severe motor needs. Studies such as that by Sawangjai et al. (1) demonstrate that automatic removal resulting from the detection of ocular artifacts in *EEG* signals using *Generative Adversarial Networks* (*GAN*) achieves precision rates exceeding 96%, enabling wheelchair control in dynamic environments.

Despite the high precision rate, the use of machine learning techniques can pose a significant challenge in the development of assistive embedded systems, as it demands devices with greater processing capacity, which, in turn, can substantially increase the final cost of the product, limiting access to this technology. Furthermore, in addition to the high computational cost, such an approach may not be feasible in certain contexts, especially in applications requiring real-time processing, thereby compromising the system's effectiveness in scenarios demanding immediate responses.

In this context, several works have already proposed blink detection systems with assistive applications. Prem *et al.* (2) developed a wheelchair controlled by blinks and brain waves, integrating *EEG* and *EOG* signals into a hybrid control system. Aziz *et al.* (3) used *Hidden Markov Models* (*HMM*) to detect blinks in *EOG* signals embedded in *EEG*, enabling automated wheelchair navigation. Paneru *et al.* (4) in turn, proposed a deep learning-based system for control based on blinks and mental commands. Although these approaches have demonstrated high accuracy, many depend on complex computational structures or prior training, hindering their application in embedded devices with limited resources. Thus, the importance of low-cost, high-computational efficiency solutions, such as the one proposed in this work, is highlighted.

Ocular Artifacts (*OA*), among other types of physiological artifacts, represent a significant challenge in the analysis of *EEG* signals. While voluntary eye actions can be interpreted as commands in Brain-Computer Interface systems, involuntary ones generate noise that compromises the accuracy of applications like neurofeedback. Methods such as wavelet transforms combined with clustering techniques have proven effective in removing these artifacts, but they have a high computational cost, making their use difficult in real-time systems.

In this work, a simplified method for blink detection in *EEG/EOG* signals is proposed, based on voltage thresholds and signal derivative analysis. The approach prioritizes computational efficiency, allowing real-time identification with experimentally validated sensitivity (*SE*) and precision (*PR*). Unlike complex methods (neural networks, wavelets), the technique avoids extensive calculations and high computational power, making it suitable for embedded systems in assistive devices. The article is organized as follows: Section 2 describes the methodology, including the hardware and the developed algorithm; Section 3 presents the experiments and results; and Section 4 discusses conclusions and practical implications.

2. Methodology

In real-world scenarios, particularly for patients with severe motor disabilities such as Amyotrophic Lateral Sclerosis (ALS) or quadriplegia, this method translates to a low-cost and non-invasive alternative for environmental interaction. By converting a simple physiological action into a reliable digital command, the proposed system can be directly integrated into smart home interfaces, virtual keyboards for communication, and accessible navigation controllers for motorized wheelchairs, democratizing access to assistive technologies.

The acquisition of electroencephalogram (*EEG*) signals constitutes a fundamental technique for monitoring and analyzing brain electrical activity. The methodology proposed in this study employs a system composed of an Arduino Nano and *AD8232*, the latter a module dedicated to capturing *electrocardiographic* (*ECG*) signals, adapted for the acquisition and processing of *EEG* or *EOG* electrical signals. Additionally, an algorithm developed for ocular blink detection is presented, based on the identification of characteristic peak and trough patterns in the captured signals, using pre-established thresholds based on the analysis of signal behavior. The processed data is visualized in real-time, allowing both storage for later analysis and the possibility of immediate *feedback*, contributing to real-time applications in the field of neuroscience and Brain-Computer Interfaces.

2.1 Hardware for Signal Acquisition and Conditioning

Table 1. Comparative table of platforms used in signal acquisition

Feature	*Arduino Uno*	*Arduino Nano*
Size	68.6 × 53.4 *mm*	45 × 18 *mm*
Processor	*ATmega328P*	*ATmega328P*
Clock Speed	16 *MHz*	16 *MHz*
Flash Memory	32 *KB*	32 *KB*
SRAM	2 *KB*	2 *KB*
EEPROM	1 *KB*	1 *KB*
Analog Inputs	6	8
Digital I/O Pins	14 (6 PWM)	14 (6 PWM)
Serial Connection	1 (Hardware)	1 (Hardware)
USB Connection	USB-B Standard	Mini-USB
Operating Voltage	5*V*	5*V*
Power Consumption	Slightly higher	Lower due to compact design
Weight	Approx. 25 g	Approx. 7 g
Typical Use	Projects requiring more pins and robustness	Compact and portable projects
Programming Port	Standard USB	Mini-USB (less robust mechanically)
Expansion	Better compatibility with shields	More limited space for shields, better for breadboards
Average Price	US$ 3.85–US$ 5.75	US$ 1.90–US$ 3.85

Table 2. *AD8232* Module Characteristics

Feature	*AD8232* Module
Function	Measure *ECG* / *EMG* / *EEG* signals
Supply Voltage	3.3*V* to 5*V*
Interface	Analog output (0 to 3.3 *V*, depending on supply) and digital pins for electrode detection (*LO+*, *LO-*)
Measurement Range	1.5*V* (relative to differential input)
Gain	Adjustable via external resistor
Filters	Integrated high-pass and low-pass filters for noise removal
Components	Operational Amplifier, Filter, Protection Circuits
Compatibility	Can be used with Arduino platforms
Power Consumption	Low, suitable for portable and battery-operated systems
Frequency Response	Optimized for biopotential signals in the 0.5–40 Hz range
Safety	Integrated protection against electrode disconnection
Applications	Wearables, biomedical research, educational projects
Support	Wide availability of libraries, tutorials, and open-source projects
Advantages	Compact, low-cost, and easy integration with microcontrollers
Size	Approximately 5 × 2.5 *cm*
Average Price	US$ 9.60–US$ 21.15

The hardware was developed with the goal of providing an accessible and efficient solution, prioritizing cost-effectiveness for signal acquisition. The Arduino Nano platform was chosen for the system due to its compact dimensions, greater number of analog inputs, equivalent processing capacity to the Arduino Uno, and reduced cost, as described in Table 1.

For the acquisition and conditioning of *EEG* signals, an approach based on *ASICs* (*Application-Specific Integrated Circuits*) was adopted, in contrast to conventional methodologies. The use of *ASICs* enables a significant reduction in circuit dimensions, favoring system portability. In this context, the use of a module based on the *AD8232* integrated circuit was chosen, which integrates amplification and filtering into

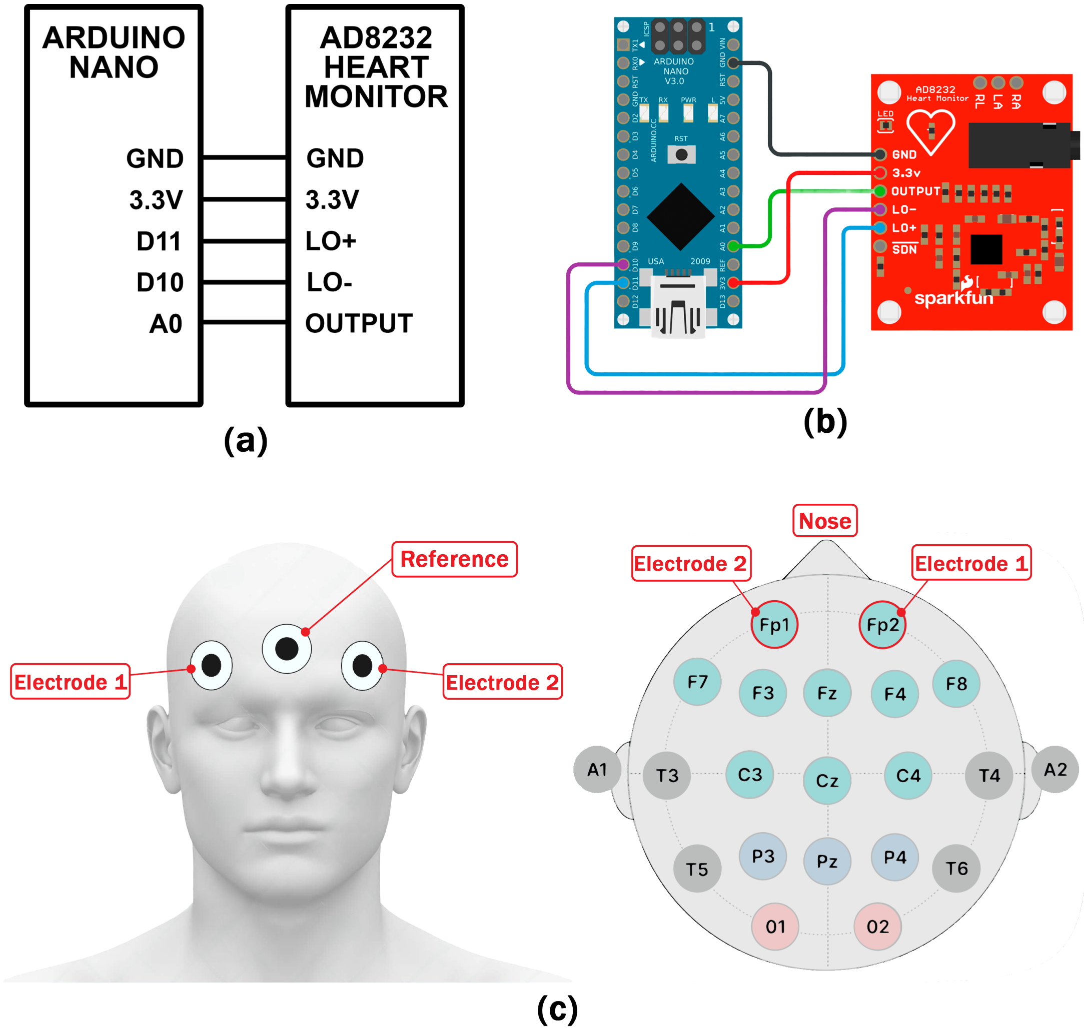

Figure 1. Connection between the *AD8232* module, the Arduino Nano, and the electrode configuration: (a) Schematic diagram of the connections between the pins of the Arduino Nano and the *AD8232* module; (b) Physical representation of the assembly with the connected modules; (c) Electrode configuration on the forehead based on the *10-20 international system*.

a single integrated circuit, with low power consumption and reduced cost (see Table 2) (5, 6).

Figure 1 presents the configuration of the electrical connections of the hardware, including the electrode connections and the physical assembly of the system. In part (a), the connection of the pins *LO+* and *LO-* to digital pins *D11* and *D10* is observed, respectively, which provide a high logic level if the electrodes disconnect from the individual. The *Output* pin of the *ASIC*, corresponding to the analog output signal, was connected directly to the analog port *A0*, allowing the transmission of the analog *EEG* signal to the microcontroller. The physical assembly of the components is shown in part (b), while the arrangement of the electrodes in the frontal region (forehead), illustrated in part (c), follows the *10-20 international system* (7).

2.2 Signal Acquisition and Ocular Artifact Detection Algorithm

The algorithm begins with the configuration of internal variables, serial communication, and the *Timer*, which is responsible for defining the signal sampling frequency. After this step, the system waits for user input via serial communication to determine the conversion scale for the read values: '*m*' for millivolts, '*n*' for nanovolts, and '*v*' for volts. With this initial configuration defined, the algorithm enters a continuous cycle, acquiring the *EEG* signal through the analog port *A0* of the Arduino Nano at a rate of *500 Hz*. This frequency was chosen based on the Nyquist theorem, considering that *EEG* signals generally range between 0.5 *Hz* and 100 *Hz* (8, 9). Thus, a new sample is read every 2 milliseconds, through the cyclic activation of a control *flag* defined by the *Timer*.

Once acquired, the signal sample passes through a moving average filter implemented with a five-position vector ($N = 5$) that acts as a low-pass filter with a cutoff frequency of 100

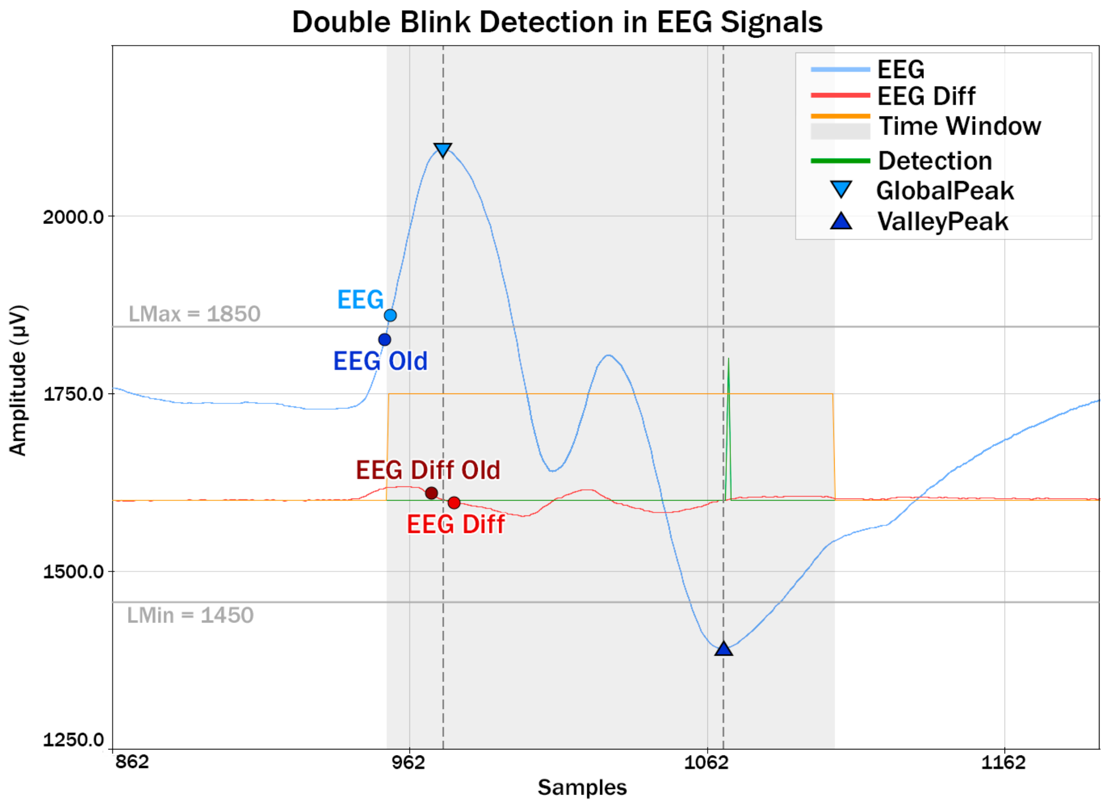

Figure 2. Double Blink Detection in *EEG* Signals: *EEG* signal (blue) with amplitude in microvolts (μV), according to the acquisition configuration. The derivative (red) and the extremes (peak, trough) are analyzed within the time window (orange and gray band). The green line indicates the detection variable. $LMax = 1850\ \mu V$ and $LMin = 1450\ \mu V$.

Hz. This filter smooths the signal, attenuating high-frequency noise that can interfere with the analysis, ensuring greater data stability for subsequent stages. Next, the filtered value is converted to the previously chosen voltage unit. Subsequently, the algorithm calculates the derivative of the *EEG* signal, an essential step to detect abrupt changes, such as the characteristic peaks and troughs of ocular artifacts.

The acquisition cycle is coordinated by a *Timer*, which operates every 2 milliseconds. Each new sample, after passing through the five-point moving average filter, has its cutoff frequency determined by the relationship between the sampling rate (F_a) and the number of samples (N), resulting in $F_c = F_a/N = 500/5 = 100$ Hz. After filtering, the signal value is converted to the previously defined voltage scale and its derivative is calculated to identify abrupt transitions in the signal. The processed data - including the filtered signal, the derivative, and detection information - are then transmitted via serial communication, allowing their visualization or storage.

The complete flowchart of this process is presented in Figure 3.

Following basic *EEG* signal processing, the ocular artifact detection algorithm seeks to identify a characteristic peak and trough pattern that indicates the occurrence of two consecutive blinks, i.e., two blinks detected within the same time window defined by the algorithm. The algorithm in question is represented in flowchart format in Figure 4.

As illustrated in Figure 4, the ocular artifact detection process begins by checking the *EEG* signal's crossing of a predefined upper threshold (*LMax*). The algorithm evaluates whether the current sample exceeds *LMax* while the previous sample (*EEG_Old*) remains equal to or below this threshold. If this condition ($EEG > LMax\ \&\& EEG\_Old \leq LMax$) is met, the *flagLMax* and *flagJanela* variables are activated (both set to 1), indicating the start of a detection window. Simultaneously, the *cont_Janela* counter is incremented to monitor the duration of the analysis window.

With *flagLMax* active, the algorithm checks the behavior of the signal's derivative (*EEG_Diff*). If the current derivative is less than or equal to zero ($EEG\_Diff \leq 0$) and the previous derivative (*EEG_Diff_Old*) was positive, a derivative zero-crossing in the descending direction is configured. This criterion validates the presence of a maximum peak, storing its value in *Peak_Global*. Next, *flagLMax* is deactivated (0), and *flagLMax_Old* is activated (1), allowing the advancement to subsequent stages.

Detection continues with monitoring inversions in the derivative signal. While *flagLMax_Old* remains active (1), the algorithm checks for sign changes in the derivative. Each valid change increments the *cont_diff* counter, which quantifies the number of extremities (peaks or troughs) detected. Simultane-

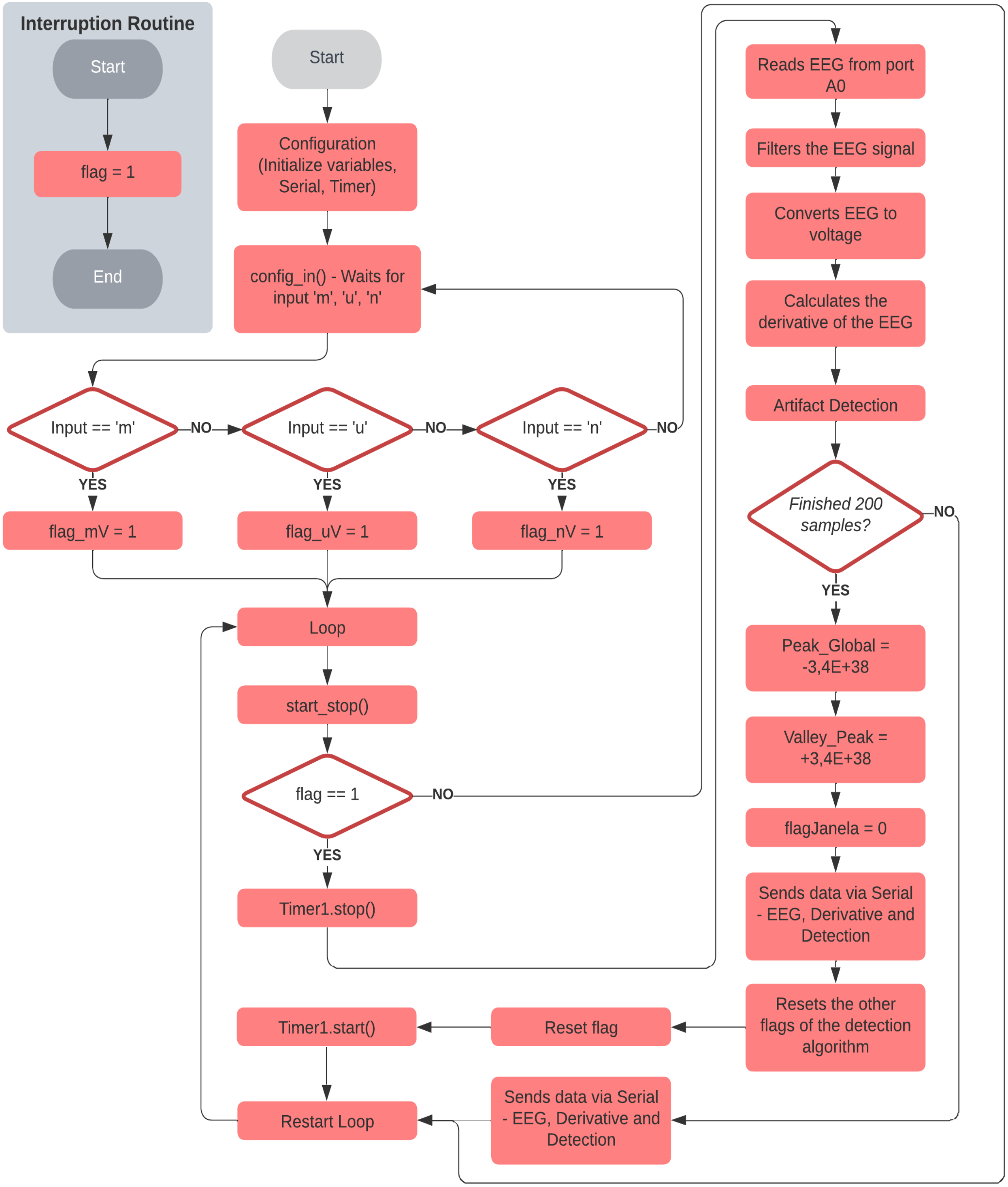

Figure 3. General algorithm for signal acquisition and ocular artifact detection used in the arduino nano.

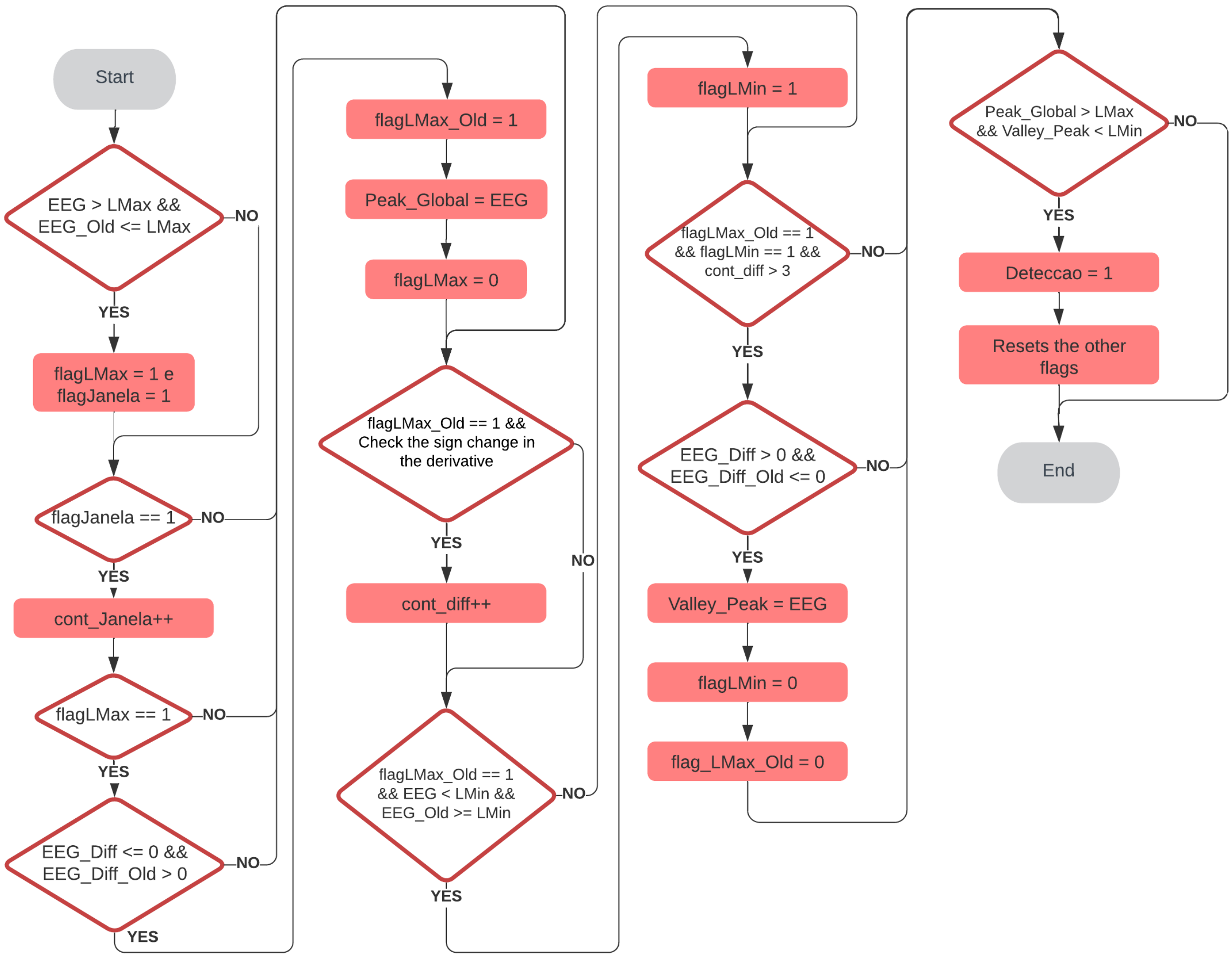

Figure 4. Ocular artifact detection algorithm used in the arduino nano.

ously, the system evaluates whether the *EEG* signal crosses the lower threshold (*LMin*) in an ascending manner, checking if the current sample is below *LMin* ($EEG < LMin$) while the previous one is equal to or above ($EEG\_Old \geq LMin$). If this condition is met, the *flagLMin* variable is activated (1).

To confirm artifact detection, the algorithm requires that *flagLMax_Old* and *flagLMin* are active (1), that the *cont_diff* counter exceeds 3 derivative sign inversions ($cont\_diff > 3$), and that the signal derivative crosses zero in the ascending direction ($EEG\_Diff > 0\ \&\& EEG\_Diff\_Old \leq 0$), validating the trough ($Valley\_Peak = EEG$). Finally, if *Peak_Global* exceeds *LMax* and *Valley_Peak* is below *LMin*, the *Detecao* variable is set to 1, indicating the identification of an ocular artifact. All *flags* (*flagLMax*, *flagJanela*, *flagLMax_Old*, *flagLMin*) and counters (*cont_Janela*, *cont_diff*) are reset, restarting the cycle.

iFigure 2 illustrates the typical behavior of the *EEG* signal during the occurrence of two consecutive blinks, highlighting the detection points. In the blue graph, the *EEG* signal is observed exceeding the upper threshold (*LMax*), characterizing the peaks associated with the blinks. The derivative of the signal, shown in red, allows for precise detection of zero-crossings, essential for the technical validation of peaks and troughs. The thresholds *LMax* and *LMin* are represented by horizontal dashed lines, serving as a reference for segmenting the events of interest. These thresholds were defined analytically, based on empirical observation of the signal behavior during testing, being adjusted manually. The values of *LMax* and *LMin* correspond to approximately 95% of the absolute maximum value and the absolute minimum value of the signal, respectively, taking a centered average of the signal around zero as a reference. Between the two peaks, a trough that crosses the lower threshold (*LMin*) is identified, completing the double blink pattern.

2.3 Algorithm Evaluation Metrics

Based on the obtained data, it is possible to calculate the precision and sensitivity of the algorithm. Precision refers to the proportion of correct detections relative to the total number of detections performed, while sensitivity reflects the algorithm's ability to identify all real blinks present in the

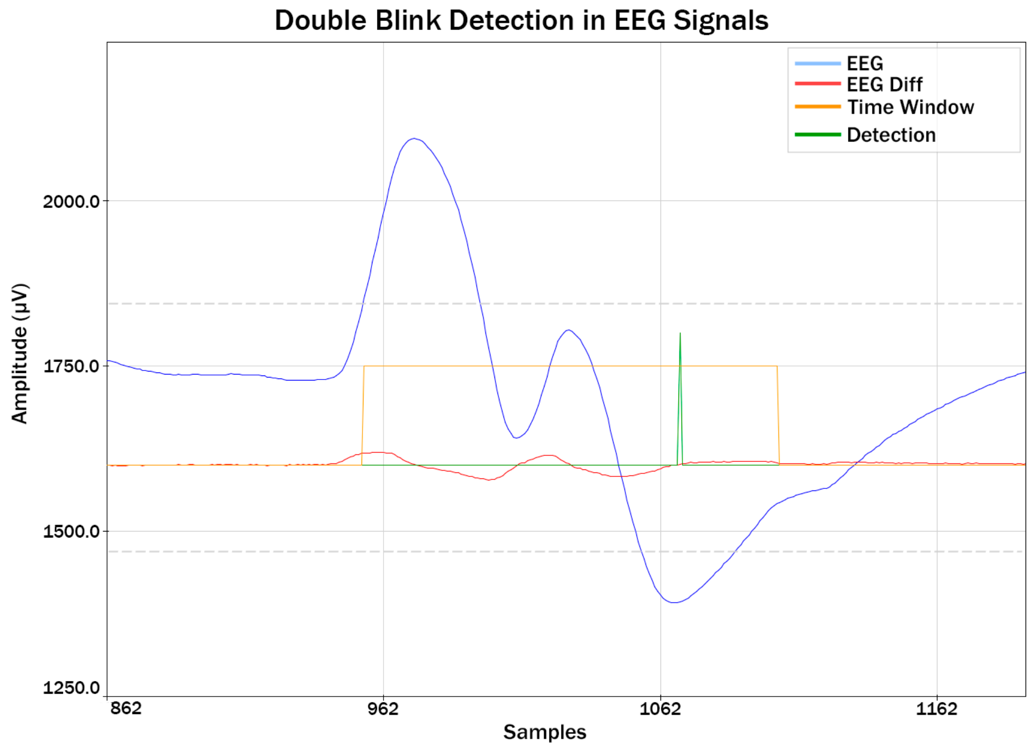

Figure 5. Example of detection performed by the method.

signal. To evaluate the algorithm's performance, the metrics of precision (*PR*) and sensitivity (*SE*) were used.

$$PR = \frac{\text{True Positives}}{\text{True Positives} + \text{False Positives}} \tag{1}$$

$$SE = \frac{\text{True Positives}}{\text{True Positives} + \text{False Negatives}} \tag{2}$$

3. Results

With the hardware and algorithms duly finalized, experimental trials with a duration of 15 minutes per session were conducted across 4 different patients, totaling 60 minutes of continuous signal acquisition. Table 3 presents the individual metrics for each patient, highlighting the variations in true positives (*TP*), false positives (*FP*), and false negatives (*FN*) due to physiological and baseline differences.

Table 3. Detection results per patient (15-minute trials) and global totals.

Patient	Total Detections	True Positives (TP)	False Positives (FP)	False Negatives (FN)
Patient 1	197	175	22	4
Patient 2	305	250	55	9
Patient 3	251	223	28	7
Patient 4	239	192	47	4
Global	**992**	**840**	**152**	**24**

In total, combining the data from all evaluation windows, the developed algorithm performed 992 detections. After a manual analysis of the signal, it was verified that 840 of these global detections corresponded to real blinks (*true positives*), while 152 were classified as false detections (*false positives*). Additionally, the algorithm failed to identify 24 real blinks across all tests (*false negatives*).

The algorithm demonstrated satisfactory performance, as illustrated in Figure 5. The figure presents the acquired raw *EEG* signal, the differential *EEG* signal (in red), and the detection signal (in green), highlighting the moment when the occurrence of an ocular artifact is confirmed.

Based on the obtained results, it was possible to calculate the precision and sensitivity of the algorithm. The precision, which represents the proportion of correct detections relative to the total number of detections performed, was approximately 84.7%. The sensitivity, which measures the algorithm's ability to identify all real blinks present in the signal (840 out of 864 total real blinks), was 97.2%.

These results demonstrate that the algorithm has robust performance in ocular artifact detection, with a high level of sensitivity. Although the precision of 84.7% is considered satisfactory, there is margin for improvement, especially in reducing *false positives*. Considering the importance of minimizing errors in practical applications, the values obtained are promising for most scenarios where it is necessary to identify blinks or ocular artifacts in *EEG* signals. The performance suggests that the algorithm is suitable for use in applications such as *Brain-Computer Interfaces* (*ICM*) or in the pre-processing of *EEG* signals for the removal of ocular artifacts.

The thresholds *LMax* and *LMin* were defined in an empirical manner, based on the analytical observation of the signal behavior during practical tests. However, adopting fixed thresholds may not be ideal in all contexts, especially considering the variability between individuals. Thus, implementing a mechanism for automatic or user-customizable adjustment represents a relevant opportunity for improvement.

In addition to algorithmic processing, the quality of *EEG* signal capture directly influences the detection accuracy. Factors such as correct electrode positioning, adequate adhesion, the use of conductive gel, and physical stability are essential for a clean signal. External interferences, such as electromagnetic noise from nearby equipment or muscle movements, can also affect data quality. However, in highly critical contexts, such as medical applications or diagnostics, where precision must be maximized, additional optimization may be necessary.

Thus, the algorithm demonstrated satisfactory performance in detecting ocular events, proving viable for practical applications. As a continuation of this work, the development of strategies aimed at reducing *false positives* is recommended, such as the introduction of dynamic adjustments in the detection thresholds through adaptive mechanisms. Furthermore, combining traditional approaches with machine learning-based methods can provide a balance between computational efficiency and precision.

4. Conclusions

This work proposes an algorithm for the detection of ocular artifacts (blinks) in real-time (*on-line*) *EEG* signals, prioritizing detection effectiveness. Its application in wheelchairs is explored as a practical example. The method presented stands out for its computational simplicity, resulting in fast and efficient processing, essential characteristics for systems operating in real-time. The algorithm demonstrates a precision of 84.7% with low latency. In contrast, more complex methods, such as the wavelet transform and k-means, tend to be slower and require greater computational capacity. Finally, it is important to emphasize that the algorithm achieved a sensitivity of 97.2%, combined with an easy-to-implement execution. By bridging the gap between clinical signal processing and embedded electronics, this proposal represents a practical, accessible, and highly efficient alternative for real-world assistive technology applications, ensuring that reliable control systems can be deployed even in resource-constrained environments.

Data Availability

To promote transparency, reproducibility, and collaborative development, the resources for this study are publicly available in our GitHub repository at: ⟨https://github.com/slaycker13/EEG-Ocular-Artifact-Detector/tree/main⟩. The repository provides the complete Arduino source code for the detection algorithm, alongside comprehensive bilingual documentation (English and Portuguese) explaining the system's logic. Additionally, it features a practical video demonstrating the real-time motor actuation triggered by ocular artifacts, illustrating the method's potential for integration into larger-scale assistive technologies, such as a motorized wheelchair control system. The repository also includes both versions of the algorithm: the standard implementation utilizing static thresholds (available in the `main` branch) and the advanced iteration featuring dynamic, adaptive thresholds.

Acknowledgements

The authors acknowledge the support of IFSul – Campus Santana do Livramento for providing support and partially funding this project. The infrastructure, resources, and encouragement offered by the institution were essential for the development, implementation, and evaluation of the proposed system. This support enabled the team to carry out experiments, acquire the necessary materials, and successfully complete the project with high technical quality.

Author Contributions

Yuri S. Pereira and Daniel D. F. Luft, as undergraduate students at IFSul, conducted the project as part of the final assignment for the Microcontrollers 2 course, including the development of hardware, implementation of the algorithm, and data acquisition. Matheus G. Tavares and Tadeu Vargas contributed by reviewing the manuscript, providing technical feedback, and assisting with the interpretation of results. Samuel S. Cardoso supervised the project, overseeing the research process, guiding the team, and providing scientific advice throughout all stages of the work.

References

[1] SAWANGJAI, P. e. a. Eeganet: removal of ocular artifacts from the eeg signal using generative adversarial networks. *Journal of Neural Engineering*, v. 26, n. 10, p. 4913–4924, 2022.

[2] PREM, S. e. a. Bci integrated wheelchair controlled via eye blinks and brain waves. In: *INTERNATIONAL CONFERENCE ON ADVANCED TECHNOLOGIES FOR SOCIETAL APPLICATIONS, 2020*. [S.l.]: Springer International Publishing, 2021. p. 321–331.

[3] AZIZ, F. et al. Hmm based automated wheelchair navigation using eog traces in eegme env. *Journal of Neural Engineering*, v. 11, n. 5, p. 056018, 2014.

[4] PANERU, B.; THAPA, B.; POUDYAL, K. N. *EEG-based AI-BCI wheelchair advancement: a brain-computer interfacing wheelchair system using deep learning approach*. 2024. Preprint (arXiv). Available at: https://arxiv.org/abs/2410.09763. Accessed on: May 29, 2025.

[5] FAVRETTO, M. A. et al. High density surface emg system based on ads1298-front end. *IEEE Latin America Transactions*, v. 16, n. 6, p. 1616–1622, 2018.

[6] JúNIOR, J. J. A. M. et al. Ad8232 to biopotentials sensors: Open source project and benchmark. *Electronics*, v. 12, n. 4, 2023.

[7] JASPER, H. H. The ten-twenty electrode system of the international federation. *Electroencephalography and Clinical Neurophysiology*, v. 10, p. 371–375, 1958.

[8] SANEI, S.; CHAMBERS, J. A. *EEG signal processing*. [S.l.]: Wiley-Interscience, 2007.

[9] BITBRAIN. *EEG amplifier: what it is, how it works and how to choose the right one*. 2021. Bitbrain Blog. Available at: https://www.bitbrain.com/blog/eeg-amplifier. Accessed on: May 29, 2025.